Applied Water Science (2019) 9:109
https://doi.org/10.1007/s13201-019-0989-6

ORIGINAL ARTICLE

Synthesis and characterization of kaolinite coated with copper oxide and its effect on the removal of aqueous Lead(II) ions

Davidson Egirani[1] · Mohd T. Latif[2] · Napoleon Wessey[1] · Nanfe. R. Poyi[3] · Shukla Acharjee[4]

Received: 8 March 2018 / Accepted: 16 May 2019 / Published online: 24 May 2019

Abstract

The removal of Lead ($Pb^{2+)}$ ions from waste water in the aquatic environment by copper oxide–kaolinite composite forms an important step involved in the reduction of Lead ions in the environment. The study investigated the synthesis, characterization, and application of copper oxide–kaolinite composite in the removal of Lead ions from aqueous systems. The synthesis of the composite involved a trimetric process to produce the copper oxide (CuO)–kaolinite composite. The characterization involved the determination of cation exchange capacity, specific surface area, and spectral analysis by sodium saturation method, nitrogen gas adsorption techniques, and scanning electron spectroscopy, respectively. The determination of parameters affecting the reaction mechanism and reaction kinetics involved the use of batch mode techniques. The findings indicated a reaction mechanism that was less than one proton coefficient, higher mass transfer rates when compared with uncoated kaolinite. Here, the intraparticle diffusion was higher than the value for the uncoated kaolinite. The reactions based on Pb^{2+} initial concentration indicated that the coated kaolinite gradually became saturated as the concentration was increased. The reactions based on solid concentration (Cp) demonstrated a complex change in the capacity of adsorption over different Pb^{2+} concentrations (10–40 mgL^{-1}) and solid concentrations (2–10 gL^{-1}). Here, the reduction in specific surface area, particle size increase, mineral aggregation, and concentration gradient effect controlled the complex changes in adsorption. In conclusion, the copper oxide–kaolinite composite significantly enhanced the adsorption of Pb^{2+} ions.

Keywords Activation · Synthesis · Characterization · Kaolinite · Pb ions · Reaction mechanism · Reaction kinetics

Introduction

The removal of Lead ($Pb^{2+)}$ ions from waste water in the aquatic environment by copper oxide–kaolinite composite forms an important step involved in the reduction of Lead ions in the environment. Therefore, the use of modified mineral absorbents has gained considerable interest. Previously, the major source of Pb^{2+} was from pigments found in Lead paints. Recently, the hydrometallurgical leaching of Cu–Pb–Zn ore to recover Cu and Zn metals releases metal load including Pb^{2+} ions into the environment (Tkacova et al. 1993; Tipre and Dave 2004). These slurries and effluents constitute an emerging source of Pb^{2+} ions into the aquatic environment and groundwater in particular. The contamination of groundwater by these slurries is through infiltration into shallow wells (Kuncoro et al. 2018; Zhang et al. 2018). These slurries and effluents containing Pb^{2+} ions are toxic to humans and the ecosystem and have attracted scientific interest (Arancibia-Miranda et al. 2016; Eric et al. 2010; Stephan et al. 2010; Dastoora and Larocpue 2004). This is

Electronic supplementary material The online version of this article (https://doi.org/10.1007/s13201-019-0989-6) contains supplementary material, which is available to authorized users.

✉ Davidson Egirani
enopmc@enopmcservices.com; eenonidavidson@yahoo.com

Mohd T. Latif
talib_latif@yahoo.com; talib@ukm.edu.my

Napoleon Wessey
napwessey@yahoo.com

Nanfe. R. Poyi
nanfe06@yahoo.com

Shukla Acharjee
sacharjee@dibru.ac.in

[1] Faculty of Science, Niger Delta University, Wilberforce Island, Nigeria

[2] School of Environmental and Natural Resource Sciences, Universiti Kebangsaan, Bangi, Malaysia

[3] Nigerian Institute of Mining and Geosciences, Jos, Nigeria

[4] Centre for Studies in Geography, Dibrugarh University, Dibrugarh, India

due to the fact that the hydrometallurgical wastes are laden with metal ions, and the pH is usually less than 5.

As a remedial measure, these wastes are stored in sealed plastic tanks under reducing condition. This process stimulates the lowering of the concentration of metals and metalloid in the slurries and leaching mud before discharge into the aquatic environment (Plescia and Maccari 1996; Tavares et al. 2017). This remedial process is dependent on the oxidation–reduction state of these metallurgical wastes and has substantial effect on the leaching of elements. However, under reducing condition the leaching metals will be negligible (van der Sloot 1991; Romero and Rincón 1999; Jha et al. 2001). Therefore, there is need to simulate in the laboratory the removal of Pb^{2+} ions from hydrometallurgical contained-slurries by using copper oxide–kaolinite composite as adsorbent.

Several methods and diverse treatment techniques have been used in the reduction in heavy metal in contaminated water (Elouear et al. 2008; Jiang et al. 2015; Ravichandran 2004; Taraba and Bulavová 2018; Olivaa et al. 2011; Chen et al. 2016, 2017, 2018; Wang et al. 2018; Uddin 2017; Cataldo et al. 2013; Strange and Onwulata 2002; Eze et al. 2013; Bouabidi et al. 2018; Maity and Ray 2018). However, some of these techniques have limited usage and the elucidations of reaction mechanisms require further attention. Consequently, innovative water purification technologies have been set and applied to remove heavy metals from water. These techniques included ion exchange (Fu and Wang 2011), membrane filtration (Blocher et al. 2003), coagulation–flocculation–sedimentation (Rivas et al. 2004), and adsorption (Husein 2013; Uddin 2017; Zaki et al. 2017). The coagulation–flocculation–sedimentation method is widely used owing to its simplicity and low cost (Rivas et al. 2004; Ndabigengesere and Narasiah 2010). However, this method will generate a large volume of sludge with low density that requires further dewatering and disposal (Haydar and Aziz 2009). The technology using membrane provides high efficiency. However, this technology has some setbacks, inclusive difficulty in maintenance. The drawback of ion exchange is the interfering of competing ions and renewal (Haydar and Aziz 2009; Hom et al. 1982).

Different from these methods, adsorption is a safe method with high effectiveness and low cost (Qiu et al. 2009; Rwiza et al. 2018; Seema et al. 2018; Amiri et al. 2018). This technique can eliminate pollutants effectively without production of harmful by-products (He et al. 2017). Saleh et al. (2017a), (b) have reported the use of activated carbon and polyzwitterionic resin to remove Lead ions from aqueous solution. Therefore, the technology of adsorption remains significant due to its efficacy and simplicity (Crini 2005). One of such emerging methods is the use of copper oxide–kaolinite composite to enhance adsorption. Drivable remediation of Lead-contaminated water using copper oxide–kaolinite composite requires comprehension of the reaction mechanism and application of appropriate kinetic models to support reaction pattern (Dzombak and Morel 1990; Lopez-Munoz et al. 2011; Chiew et al. 2016).

In adsorption, several factors are known to control the reaction mechanism and reaction kinetics of Lead removal from the environment. These factors include metal speciation, metal mobility, sizes of adsorbent, adsorbent surface charge, adsorbent surface area, and chemistry of proton–metal ratio (Arancibia-Miranda et al. 2016). The contact time and pH are regulating factors in the hydrolysis of Lead ions and species solubility (Zhengn et al. 2018; Maruthupandy et al. 2017; Kuncoro et al. 2018). These parameters enhance the reorganization of reactive sites (Wang et al. 2018). The particle concentration, particle sizes, and chemistry of the adsorbent control the diminution of Lead removal from the aquatic environment (Akpomie et al. 2015). A kaolinite coated with aluminum on its surfaces is known to reduce adsorption (Keren 1986; Karickhoff and Bailey 1973). Outer-sphere complexation is linked to increase Lead removal as adsorbent particle concentration was increased. However, the increase in particle size and particle concentration does not necessarily result in an increase in Pb^{2+} uptake all the time (Eze et al. 2013). The quantitative decrease in adsorption and vice versa is dictated by the increase in metal concentration (Akpomie et al. 2015; Hua et al. 2012). The four successive steps have been identified as pathway for a solid solution system undergoing adsorption. These include: external mass transfer, intraparticle diffusion, protonation, and adsorption of molecules of sorbate (Uddin 2017; Shen et al. 2017, 2018). The fast process of intraparticle diffusion and slow process of outer-sphere complexation are components of the reaction mechanism involved in Lead uptake in aqueous solution (Bonnet et al. 2017; Dhal et al. 2013; Khodadadi et al. 2017). In addition, Lead removal from the aquatic environment is controlled by solution concentration and exchange of ions (Egirani and Wessey 2015a; Wang et al. 2016).

The use of untreated kaolinite in Lead removal formed the focus of the previous studies (Egirani and Wessey 2015a, b). An untreated kaolinite possesses the capacity to adsorb heavy metals. This comes from cation exchange and inner-sphere complexes formation via the aluminol and silanol sites (Allahdin et al. 2017, Akpomie et al. 2015). Recent studies reported the use of CuO coating supported by kaolinite to treat Lead ions in aqueous solution (Egirani et al. 2017a, b). Here, the authors have used the same experimental conditions to investigate the effect of CuO–kaolinite composite in the removal of Lead ions in aqueous media. This was in relation to pH, contact time, Lead initial concentration, and prolonged contact time. The experiments were conducted using batch mode-related techniques under reducing condition. The synthesis of the adsorbent, characterization

of the adsorbent, and the testing of copper oxide-coated kaolinite to remove Lead ions have been discussed.

Materials and experimental methods

Adsorbent characterization

In this paper, Richard Baker Harrison Kaolinite obtained from Richard Baker Harrison Company in the UK is denoted as RBH kaolinite. Suspension pH of RBH kaolinite and pH of solutions were determined using the Model 3340 Jenway ion meter. The cation exchange capacity (CEC) was evaluated by Na saturation method. Standard volumetric Brunauer, Emmett, and Teller (BET) method was used to determine the specific surface area of the RBH kaolinite (Brunauer et al. 1938). This was done by measuring the adsorption of N_2 gas on the mineral surface at the boiling point of liquid nitrogen (Lowell and Shields 1991). The spectral analysis was done using a JEOL JSM 5900 LV Scanning Electron Microscopy (SEM) with Oxford INCA Energy Dispersive Spectroscopy (EDS) (Karickhoff and Bailey 1973; Janaki et al. 2014). The adsorbent samples were viewed, and images of secondary electron were acquired at low vacuum control pressure. A standard laboratory procedure was used to determine the point of zero salt effect (PZSE) of the RBH kaolinite. This procedure was carried out using potentiometric titration that was conducted after equilibration of 1% (by mass) of RBH kaolinite suspensions (Alves and Lavorenti 2005; Bolan et al. 1986). A 1:1 electrolyte solution was initially adjusted to pH ranges near the PZSE and used as reference.

Synthesis of copper oxide–RBH kaolinite composite

The procedure was as previously reported (Eren 2009; Phiwdang et al. 2013; Egirani et al. 2017a, b). About 20 g of RBH kaolinite was mixed with 100 mL 1 M $Cu(NO_3)_2$ solution and 180 mL of 2 M NaOH solution. These were freshly prepared, and the reaction mixture was maintained at 90 °C for 48 h. The RBH kaolinite activated with the NaOH solution was dispersed into 150 mL of 0.10 M $Cu(NO_3)_2$ solution. 0.10 M NaOH aqueous solution of three hundred microliters was titrated at the rate of 1 mL/h. Carbonate salt formation was minimized, by titrating under nitrogen flow condition (Maruthupandy et al. 2017). To free the content from NO_3^- ions, precipitate centrifugation and washing were carried out. Copper oxide-coated kaolinite solid was formed after heating the content for 4 h in air at 700 K. Adsorbent was verified from the X-ray diffraction (XRD) patterns of the product.

Batch mode adsorption experiments

This stock solution contains 100.0 mg/L Pb. 10 mL, 15 mL, 20 mL, and 40 mL of the stock solution were dispensed directly into a 100.0-mL volumetric flask to prepare the 10 mg/L, 15 mg/L, 20 mg/L, and 40 mg/L standards. These standards were treated with 2 g/L, 4 g/L, 6 g/L, 8 g/L, and 10 g/L of the copper oxide–montmorillonite composites made onto 50 mL. A 0.2-µm pore size cellulose acetate filter was used on the supernatant and content analyzed for Pb^{2+} ions left in solution, using a Hitachi Atomic Absorption Spectrophotometer (HG-AAS). The Pb^{2+} solutions (10–40 mgL^{-1}) were reacted with 1% each of RBH copper oxide-coated kaolinite suspension. To determine the effect of metal initial concentration, the suspension was made unto 50 mL and subsequently equilibrated for 24 h at pH = 4–8. Here, only results at pH = 4 have been reported for mimicking the scenario in hydrometallurgical contained-waste in reducing condition. A range of solid concentrations of copper oxide-coated kaolinite (2 gL^{-1}, − 10 gL^{-1}) made unto 50 mL were reacted with solutions containing Pb(II) ions (10–40 mgL^{-1}) and equilibrated for 24 h at pH = 4–8. This was used to investigate particle concentration effect (Cp). Lead concentrations (10–40 mgL^{-1}) were reacted with 1% RBH copper oxide-coated kaolinite at pH = 4 to 8. The suspensions were made unto 50 mL and aged from 24 to 720 h. These were equilibrated for 24 h at pH = 4–8, and the content was securely sealed and kept in the dark to avoid oxidation and leaching of CuO–kaolinite interface (Pirveysian and Ghiaci 2018). This was used to investigate the effect of aging. All experiments in triplicates were conducted at ambient temperature in reducing condition. Kinetic experiments were carried out, to deduce the reaction mechanisms involved in Lead removal using several kinetic models. The proton coefficient otherwise known as the proton exchange isotherm was derived from change of pH versus Log Kd plot. This was based on Freundlich isotherm (Egirani and Wessey 2015b; Wang et al. 2016) as given by Eqs. (1, 2):

$$\propto \mathrm{SOH} \leftrightarrow \mathrm{SO}^- + \propto \mathrm{H}^+ \ldots \quad (1)$$

$$\mathrm{LogKd} = \mathrm{Log}(\mathrm{Kp}\{\mathrm{SOH}\}^{\alpha}) + \alpha\mathrm{pH} \quad (2)$$

Here, SOH equals the mineral surface binding site, SO^- equals the soluble arsenite species, $\log K_p$ equals the apparent equilibrium binding constant, and α equals the coefficient of protonation. This represents the number of protons displaced when one mole of metal binds to the mineral surface (Egirani and Wessey 2015a; Contescu et al. 1993; Arshadi et al. 2014). The plot of logKd versus pH provided the slope as the proton coefficient. To determine this coefficient, 1% RBH copper oxide-coated kaolinite suspension was regulated to required pH. This was made unto 50 mL and reacted with Lead

ion solution of 10 mgL^{-1}. Secondly, the mass transfer rate and intraparticle diffusion were derived from Eqs. (3, 4, 5):

$$Q_t(mgg^{-1}) = [C_o - C_t]^V/_m \quad (3)$$

Here, Co equals the initial Lead concentration (mgL^{-1}) at time $t=0$; C_t equals the concentration (mgL^{-1}) at time t; V equals the total copper oxide-coated kaolinite suspension volume; and m is the weight of the sorbent (g) (Egirani and Wessey 2015a; Uddin 2017). The kinetics of adsorbate to the mineral surface binding sites was controlled by the mass transfer constant K_f. Here, C_t/C_0 versus time provided the slopes of the curves derived from Eq. (4) (Hua et al. 2012; Egirani and Wessey 2015a):

$$\left[\frac{d\left(C_t/C_0\right)}{dt}\right]_{t=0} \cong -K_f S_s \quad (4)$$

Here, C_t and C_0 denote the initial concentrations of Pb^{2+} at time t, S_s equals the exposed specific surface area of the adsorbent, and Kf denotes the coefficient of mass transfer (Sharifpour et al. 2018). These models as reviewed by Qiu et al. (2009) and derived from the Freundlich isotherm were adopted to describe sorption of Pb^{2+} ions. These models were considered appropriate for heterogeneous surfaces over a wide range of solute concentrations (Uddin 2017; Liu et al. 2018). To investigate the action of intraparticle diffusion on Pb^{2+} adsorption, the Weber–Morris model was used (Feng et al. 2004; Tavares et al. 2017; Uddin 2017) as given in Eq. (5):

$$Q_t = K_i t^{0.5} + C \quad (5)$$

Here, K_i equals the intraparticle diffusion constant (mg/g min) and the intercept (C) represents the effect of the layer boundary. K_i value is derived from slope (K_i) of the plots of Q_t versus $t^{0.5}$. A linear plot of Q_t versus $t^{0.5}$ indicates that diffusion of intraparticle was involved in the process of adsorption. The rate-controlling step was regulated by intraparticle diffusion, if these lines pass through the origin. Otherwise, this is indicative of some degree of boundary layer control (Nguyen et al. 2015; Taghipour et al. 2018).

The equilibrium adsorption capacity ($q_{e\,mgg}^{-1}$) and adsorption percentage (%) were calculated from Eqs. (6, 7):

$$Q_e(mgg^{-1}) = [C_0 - C_e]^V/_m \quad (6)$$

$$\text{Adsorption efficiency} = \left(\frac{C_0 - C_e}{C_0}\right) \times 100 \quad (7)$$

where C_0 and C_e (mgg^{-1}) are the final equilibrium concentrations of Pb^{2+} ions in solution, V(mL) is the volume of solution, and m(mg) is the adsorbent mass.

Table 1 Summary of adsorbent (kaolinite) characterization (Egirani et al. 2017a)

Components of characterization	Values
SiO_2 (%)	47.00 ± 0.03
Al_2O_3 (%)	38.00 ± 0.05
Moisture content (%)	1.50 ± .01
Specific gravity	2.60 ± 0.04
Water-soluble salt (%)	0.20 ± 0.05
CEC (mmols/g)	170.00 ± .01
% (< 1000 nm) colloid	3.00 ± 05
Particle size range (μm)	0.60–20.01 ± 0.05
pH ± σ	6.05 ± 0.05
Surface area (SSA ± σ) (m^2/g)	47.01 ± 0.024
Point of zero salt effect (PZSE)	7.00 ± 0.01

For these reaction mechanisms, 1% copper oxide-coated kaolinite was reacted with 10 mgL^{-1} Pb^{2+} ion solution. The content was made unto 50 mL and regulated to a range of pHs (pH = 4–8). The amount of Pb^{2+} ions remaining in solution was determined after 2nd h, 4th h, 6th h, 8th h, 12th h, 18th h, and 24th h. These experiments were conducted in triplicates at ambient temperature. A 0.2-μm pore size cellulose acetate filter was used on the supernatant, and content was analyzed for Pb^{2+} ions, using a Hitachi Atomic Absorption Spectrophotometer (HG-AAS).

Results

In this study, the RBH kaolinite contained SiO_2, 47 (%), Al_2O_3 18 (%), with moisture content 1.5 (%), specific gravity 2.6, water-soluble salt 0.20 (%), CEC 170.00 (mmols/g), colloid 3.00 (%), particle size range 0.600–20.01 (μm), pH = 6.05, specific surface area 47.01 (m^2/g), 56.00 and 7.00 point of zero salt effect. The adsorbent involved in this study has been characterized and is summarized in Table 1 and Figs. 1, 2, 3, 4). The X-ray diffraction spectrum indicated kaolinite as the key constituent. The EDS spectrum and SEM morphology indicated the presence of kaolinite and copper oxide. The point zero charges pHpzc (i.e., point of zero salt effect) and the specific surface area are characteristics of the mineral surface. At the pHpzc, the negative charges on the mineral surface equal the positive charges. Therefore, this determines the positive and negative charges divide the mineral surface. These table and figures confirm kaolinite as the key mineral and copper oxide–kaolinite composite as the synthetic product.

The proton coefficient (α) was based on a theoretical framework given by Eqs. (1, 2), predicted and derived from the plot (Fig. 5) and Table 2. The value was 0.02, < 1. The intraparticle diffusion was based on a theoretical framework

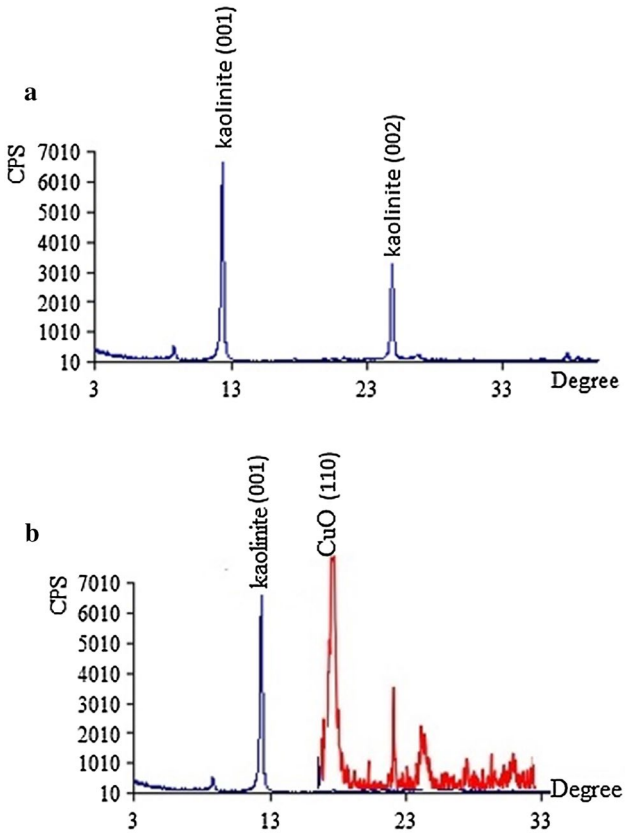

Fig. 1 **a** X-ray diffraction of kaolinite (Egirani et al. 2017a), **b** X-ray diffraction of synthetic copper oxide–kaolinite showing peaks

given by Eq. (5), predicted and derived from the plot (Fig. 6) and Table 3. The intraparticle diffusion constant derived from the slope was 13.346 (mgg^{-1}) $min^{0.5}$, and the intercept C was 448.64, $\neq 0$. This plot consisted of two linear parts, with the first part representing the external mass transfer. The S-curve adsorption pattern plateaued after 720th minute. The second part of this plot represented the intraparticle diffusion.

The mass transfer rate predicted from Eqs. (3, 4) and derived from Fig. 1 (in Supplementary material) is given (Table 1 in Supplementary material). Also, this consisted of two linear parts, with the first part higher than the second. The second linear part started after the 15th h. Figure 2 (in Supplementary material) consists of three linear parts. There was a decrease in capacity of adsorption as Pb^{2+} initial concentration was increased. Adsorption capacity decreased from 3286 to 596.1895 mgg^{-1}, over the range of Pb^{2+} concentrations investigated. The maximum adsorption capacity occurred at 10 mgL^{-1}. Figure 3 (in Supplementary material) consists of three linear parts occurring in a complex pattern. With 40 mgL^{-1} initial metal concentration, there was a decrease in capacity of adsorption as particle concentration was increased unto

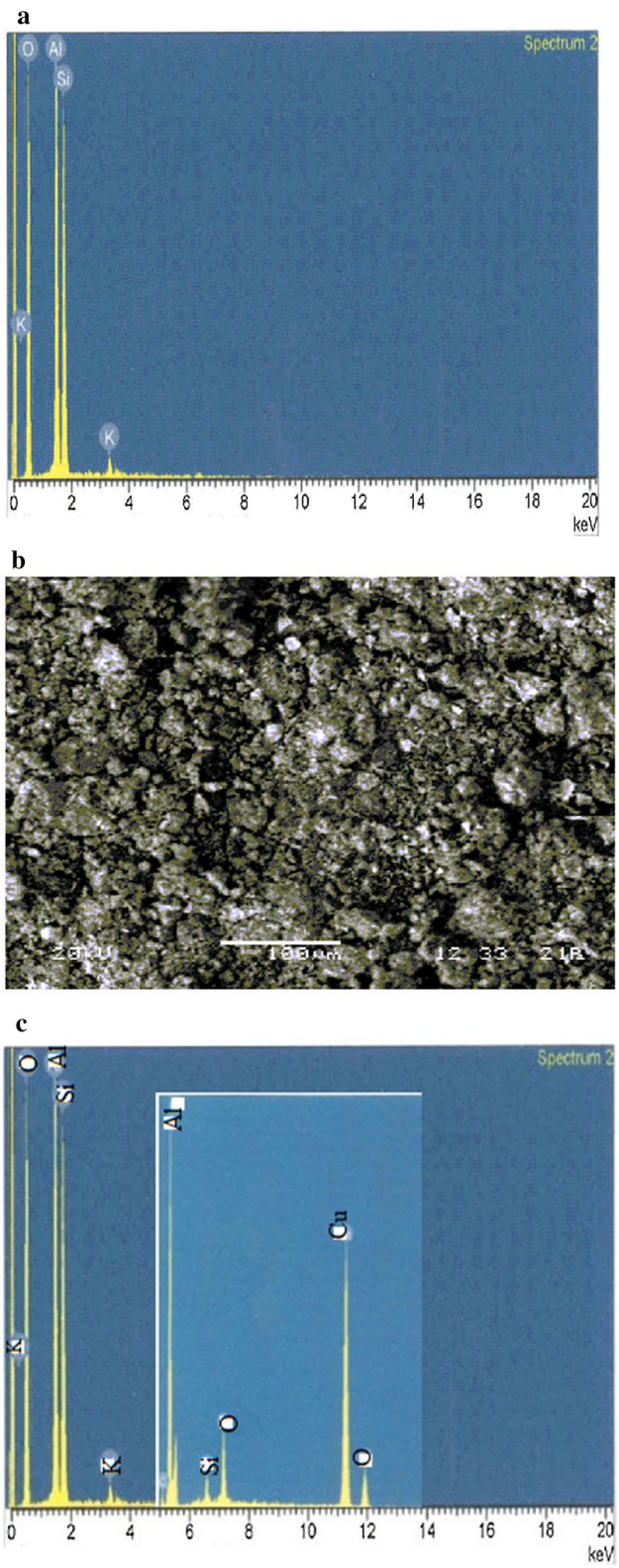

Fig. 2 **a** EDS for kaolinite showing element peaks (Egirani et al. 2017a), **b** SEM for CuO–kaolinite composite showing particle sizes (Egirani et al. 2017a), **c** EDS for CuO–kaolinite composite showing element peaks

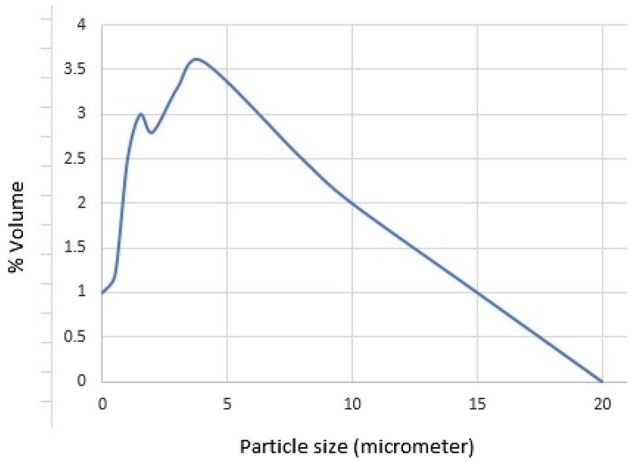

Fig. 3 Particle size distribution of kaolinite

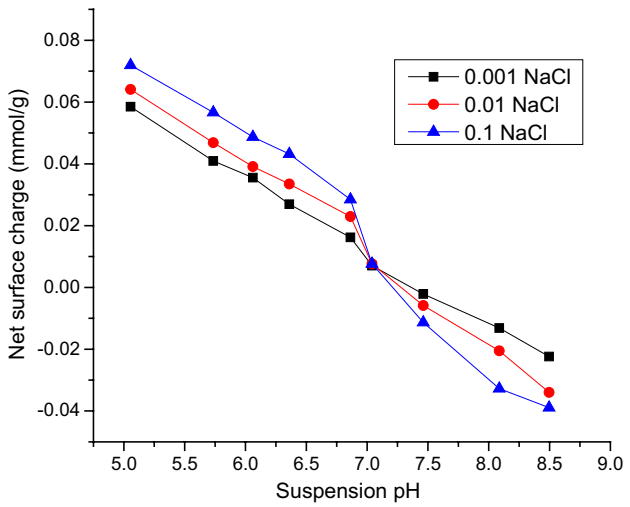

Fig. 4 Point of zero salt effect of kaolinite (Egirani et al. 2017a)

8 gL^{-1}; thereafter, it decreases as solid concentration was increased unto 10 gL^{-1}. The highest adsorption capacity was at 40 gL^{-1}. Adsorption capacity at 10 mgL^{-1} was the lowest over the range of initial metal concentrations investigated (10–40 $mgL^{-1)}$. The prolonged contact time (i.e., aging) increased with an increase in adsorption capacity. This adsorption plot consisted of one linear part, and the capacity of adsorption increased from 902 to 932 mgL^{-1} (Fig. 4 in Supplementary material). The rate of removal of Pb^{2+} ions increased from 570 to 870 mgg^{-1} over the range of residence times investigated. The adsorption capacity generally increased with the increase in pH. The adsorption efficiency increased from 84 to 86% over the range of pHs investigated (Fig. 5 in Supplementary material).

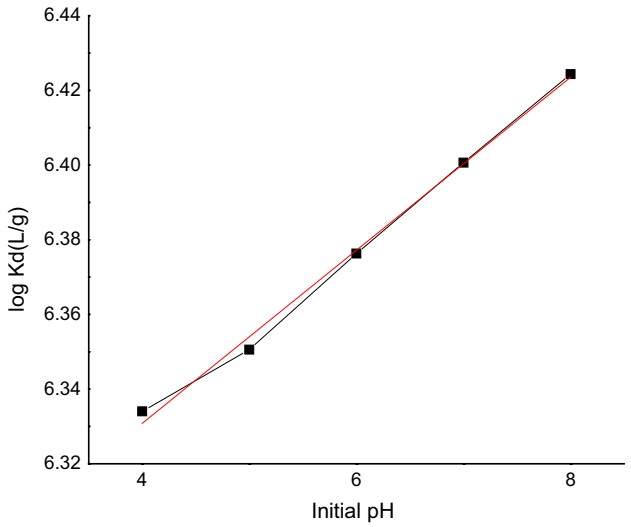

Fig. 5 Plot of Log Kd (distribution coefficient) versus final pH for CuO–kaolinite composite used for the determination of proton coefficient

Table 2 Statistical presentation of proton coefficient for CuO–kaolinite composite derived from Fig. 5

Equation		$Y=a+b*x$
Proton coefficient α		0.023
	Value	SE
Log Kd (L/g)		
Intercept	6.230	4.51^{-6}
Slope	0.023	7.32^{-7}

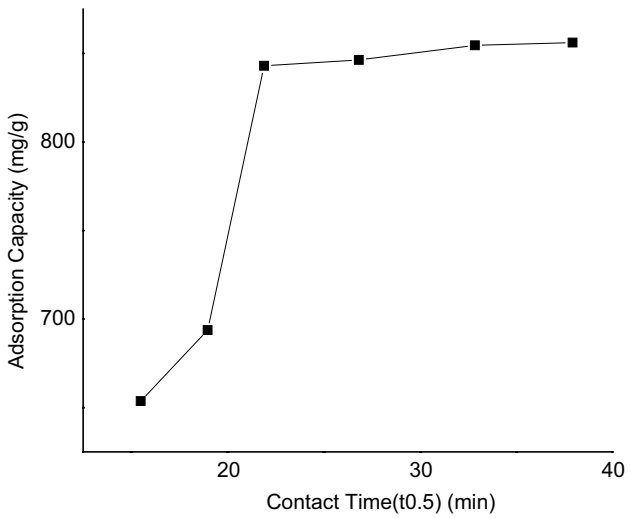

Fig. 6 Plot of adsorption capacity versus time for CuO–kaolinite composite used for the determination of intraparticle diffusion

Table 3 Statistical presentation of intraparticle diffusion data for CuO–kaolinite composite derived from linear fit of Fig. 6

Equation	$Y=a+b*x$	
	Value	SE
Q_t (mgg^{-1}) $min^{0.5}$		
Intercept	448.646	0.005
Slope	13.346	2.046^{-4}

Discussion

The proton coefficient, intraparticle diffusion, and mass transfer rates were used to discuss the reaction mechanism. In the previous studies deprived of coated copper oxide on kaolinite, proton coefficient was greater than one (Egirani and Wessey 2015a; Wang et al. 2016). Here, the α for copper oxide-coated kaolinite was less than one (Table 2). This suggested that protonation was not the controlling factor in the adsorption of Pb^{2+} ions by the copper oxide–kaolinite. There was an indication that protonation was lowered in the presence of copper oxide coating. A coated medium could mask the sites of acidity on the edges and planar surfaces of kaolinite. Intraparticle diffusion was involved in the adsorption process (Fig. 6 and Table 3). However, this reaction was not rate limiting. Also, there was an indication of boundary layer control. When compared with the previous studies (Egirani and Wessey 2015a, b), the slope and intercept for the uncoated kaolinite were lower than the coated kaolinite, thus suggesting that the presence of copper oxide coating enhanced intraparticle diffusion. Further comparison with the previous studies revealed that the mass transfer rates for the coated kaolinite were higher than results for the uncoated kaolinite (Egirani and Wessey 2015a). Thus, there was enhancement of mass transfer of adsorbate to the external layer of the adsorbent (Fig. 1 in Supplementary material). Based on the plot of adsorption capacity versus time, it was obvious that Pb^{2+} adsorption was dependent on contact time (Fig. 6). The dependent on time attribute of Pb^{2+} removal was assessed from 2 to 24 h at ambient temperature. This was at initial Pb^{2+} concentration of 10 mgL^{-1} at pH = 4–8. Here, only results at pH = 4 were discussed. This reaction pattern plateaued after the 12th h at 843 mgg^{-1}.

Based on Fig. 6, the capacity of adsorption increased with the increase in contact time and the optimum adsorption (i.e., 856 mgg^{-1}) was at the 24th h. The adsorption rate was initially fast, and the capacity of adsorption increased over time. The initial speedy adsorption of Pb^{2+} ions in the first reaction step may be ascribed to larger numbers of active adsorption sites and was related to outer-sphere complexation (Hua et al. 2012; Tavares et al. 2017). The investigation of different metal concentrations was relevant in this report because most contaminated aquatic systems offer different concentrations of Pb^{2+} ions. The decrease in adsorption capacity of the coated kaolinite as Pb^{2+} concentration was increased indicated that the active and reactive sites of the RBH copper oxide-coated kaolinite were not yet saturated (Fig. 2 in Supplementary material). Egirani and Wessey (2015a) reported a similar decrease in Pb^{2+} adsorption as initial concentration was increased for copper oxide-coated kaolinite. Again, for Pb^{2+} ions adsorbed on uncoated kaolinite, adsorption decreased with the increase in metal concentration. It could be suggested that the mass transfer rate of metal ions between the solid solution phases was controlled by pressure gradient. Here, the numbers of active sites are fixed and became limited as Pb^{2+} ions were adsorbed. Akpomie and others (Akpomie et al. 2015) reported a similar decrease in adsorption capacity for some heavy metals adsorbed on montmorillonite as the metal initial concentration was raised from 100 to 300 mgL^{-1}. In this report, there was change in linear plot, after the 10 mgL^{-1} point. Thus, this indicated a gradual plateauing of the capacity of adsorption due to gradual saturation of the active and reactive sites.

The complex characteristics of adsorption over the range of Cps investigated were different from the report of Egirani and Wessey (2015a). In this case, the increase in concentration of particle led to a complex adsorption process. The decrease in adsorption capacity suggested an increase in particle size and aggregation of the mineral system as the reaction proceeded. In addition, there was a decrease in the specific surface area and the reactive sites on the surfaces of RBH copper oxide–kaolinite. Again, an increase in adsorption as recorded at some metal concentration may be assigned to pressure gradient effect, due to increased Kp effect (Eq. 2). This characteristic means that for every reaction pressure exacted on the system due to binding constant Kp, there was a corresponding pressure gradient effect on the system. 40 mgL^{-1} Pb^{2+} concentration provided the highest adsorption capacity of 3286 mgg^{-1}, and 10 mgL^{-1} offered the lowest adsorption capacity of 596 mgg^{-1}. Thus, there was indication that the latter metal concentration was the minimum for minimal adsorption capacity of Pb^{2+} ions in this regard.

In the previous studies by Egirani and Wessey (2015a), (b), there was a similar increase in adsorption capacity as aging was increased (Fig. 4 in Supplementary material). This characteristic was for the same range of residence times investigated. In this report, the adsorption capacity was higher over the same range of residence times investigated. This higher magnitude was essentially controlled by hydrolysis and reactive support of copper oxide coating. Because Pb^{2+} removal was pH dependent, investigation of this was necessary in this report. The protonation and hydroxylation of a mineral surface controlled the adsorption process as pH was increased (Fig. 5 in Supplementary

material). This characteristic was similar to an earlier report by Egirani and Wessey (2015a). Also, Akpomie et al. (2015) revealed a similar trend for adsorption of heavy metals on uncoated montmorillonite. As pH was increased, there was a decrease in protonation and enhancement in hydroxylation. This process favored Pb^{2+} adsorption. The huge amount of quantities of protons competed with the Pb^{2+} ions for reactive and active sites at low or acidic pH. However, there was a decrease in the number of available protonation sites as pH was increased. This gave rise to an increase in hydroxylation on the copper oxide-coated kaolinite surfaces.

Conclusions

In this paper, the synthesis and characterization of copper oxide–kaolinite composite and its effect on the removal of Lead have been investigated. The synthesis involved a trimetric process to produce the copper oxide (CuO)–kaolinite composite. The characterization involved the determination of cation exchange capacity, specific surface area, and spectral analysis by sodium saturation method, nitrogen gas adsorption techniques, and scanning electron spectroscopy, respectively. The determination of parameters affecting the reaction mechanism and reaction kinetics involved the use of batch mode techniques. The reaction mechanism of adsorption tested included proton coefficient that was less than one, intraparticle diffusion that was controlled by boundary layer, and mass transfer rates that were higher than those of bare kaolinite. There was a decrease in adsorption capacity as Pb^{2+} concentration was increased, thus indicating that the active and reactive sites of the copper oxide-coated RBH kaolinite were not yet saturated. The complex characteristics of adsorption over the range of Cps investigated indicated that for every reaction pressure exacted on the system due to adsorption, there was a corresponding pressure gradient effect on the system. The decrease in adsorption capacity in this scenario suggested an increase in particle size and aggregation of the adsorbent system as the reaction proceeded. The higher magnitude of adsorption when compared with the previous studies indicated that adsorption was essentially controlled by hydrolysis, reactive support of copper oxide coating, and increased reorganization of active sites. Here, the adsorption efficiency increased from 84 to 86% over the range of pHs investigated. As the pH was increased, there was a decrease in protonation and enhancement of hydroxylation. This characteristic led to an increase in adsorption capacity the copper oxide–kaolinite composite. Therefore, the presence of copper oxide coating on kaolinite enhanced the reorganization of active sites and increased the adsorption of Pb^{2+} ions.

Acknowledgements The authors are grateful to authorities of the corresponding author for the release of SL20172018 research allowances used for this project.

References

Akpomie KG, Dawodu FA, Adebowale KO (2015) Mechanism on the sorption of heavy metals from binary-solution by a low-cost montmorillonite and its desorption potential. Alex Eng J 54:757–767

Allahdin O, Mabingui J, Wartel M, Boughriet A (2017) Removal of Pb2 + ions from aqueous solutions by fixed-BED column using a modified brick: (Micro)structural, electrokinetic and mechanistic aspects. Appl Clay Sci 148:56–67

Alves ME, Lavorenti A (2005) Point of zero salt effect: relationship with clay mineralogy of representative soils of Sao Paulo State, Brazil. Pedosphere 15:545–553

Amiri MJ, Arshadi M, Giannakopoulos E, Kalavrouziotis IK (2018) Removal of mercury(II) and lead(II) from aqueous media by using a green adsorbent: kinetics, thermodynamic, and mechanism studies. J Hazard Toxicol Radioact Waste 22:04017026

Arancibia-Miranda N, Baltazar SE, García A, Mũnoz-Lira D, Sepúlveda P, Rubio MA, Altbir D (2016) Nanoscale zero valent supported by zeolite and montmorillonite: template effect of the removal of lead ion from an aqueous solution. J Hazard Mater 301:371–380

Arshadi M, Soleymanzadeh M, Salvacion JWL, SalimiVahid F (2014) Nanoscale zero-valent iron (NZVI) supported on sineguelas waste for Pb(II) removal from aqueous solution: kinetics, thermodynamic and mechanism. J Colloid Interface Sci 426:241–251

Blocher C, Dorda J, Mavrov V, Chmiel H, Lazaridis NK, Matis KA (2003) Hybrid flotation—membrane filtration process for the removal of heavy metal ions from wastewater. Water Res 37:4018–4026

Bolan NS, Syers JK, Tillman RW (1986) Ionic strength effects on surface charge and adsorption of phosphate and sulphate by soils. Eur J Soil Sci 37:379–388

Bonnet M-L, Costa D, Protopopoff E, Marcus P (2017) Theoretical study of the Pb adsorption on Ni, Cr, Fe surfaces and on Ni based alloys. Appl Surf Sci 426:788–795

Bouabidi ZB, El-Naas MH, Cortes D, McKay G (2018) Steel Making dust as a potential adsorbent for the removal of Lead (II) from an aqueous solution. Chem Eng J 334:837–844

Brunauer S, Emmett PH, Teller E (1938) Adsorption of gases in multimolecular layers. J Am Chem Soc 60:309–319

Cataldo S, Gianguzza A, Pettignano A, Villaescusa I (2013) Lead(II) removal from aqueous solution by sorption onto alginate, pectate and polygalacturonate calcium gel beads. A kinetic and speciation based equilibrium study. React Funct Polym 73:207–217

Chen Y-M, Gao J-B, Yuan Y-Q, Maa J, Yu S (2016) Relationship between heavy metal contents and clay mineral properties in surface sediments: implications for metal pollution assessment. Cont Shelf Res 124:125–133

Chen G, Shah KJ, Shia L, Chiang P-C (2017) Removal of Cd(II) and Pb(II) ions from aqueous solutions by synthetic mineral adsorbent: performance and mechanisms. Appl Surface Sci 409:296–305

Chen Y, Ho S-H, Wang D, Wei Z-S, Chang J-S, Ren N-Q (2018) Lead removal by a magnetic biochar derived from persulfate-ZVI treated sludge together with one-pot pyrolysis. Bioresour Technol 247:463–470

Chiew CSC, Yeoh HK, Pasbakhsh P, Krishnaiah K, Poh PE, Tey BT, Chan ES (2016) Halloysite/alginate nanocomposite beads: kinetics, equilibrium and mechanism for Lead adsorption. Appl Clay Sci 119:301–310

Contescu C, Jagiello J, Schwarz JA (1993) Heterogeneity of proton binding sites at the oxide/solution interface. Langmuir 9:1754–1765

Crini GG (2005) Recent developments in polysaccharide-based materials used as adsorbents in wastewater treatment. Prog Polym Sci 30:38–70

Dastoora AP, Larocpue Y (2004) Global circulation of atmospheric lead: a modeling study. Atmos Environ 38:147–161

Dhal B, Thatoir HN, Das NN, Paudey BD (2013) Chemical and microbial remediation. J Hazard Mater 250–251:272–292

Dzombak DA, Morel F (1990) Surface complexation modeling: hydrous ferric oxide. Wiley, New York, pp 443–468

Egirani DE, Wessey N (2015a) Effect of clay and goethite mineral systems on lead removal from aqueous solution: paper ii. Int J Multidiscip Acad Res 3:83–92

Egirani DE, Wessey N (2015b) Effect of mineral systems on Lead removal from aqueous solution: part I. Asian J Basic Appl Sci 2:61–73

Egirani DE, Latif MT, Poyi NR, Wessey N, Acharjee S (2017a) Synthesis and characterization of kaolinite coated with copper oxide and its effect on the removal of aqueous mercury(ii) ions: part ii. Int Res J Chem Chem Sci 4:043–048

Egirani DE, Latif MT, Poyi NR, Wessey N, Acharjee S (2017b) Synthesis and characterization of kaolinite coated with copper oxide and its effect on the removal of aqueous mercury(ii) ions: parti. Int Res J Chem Chem Sci 4:055–061

Elouear Z, Bouzid J, Boujelben N, Jamoussi M, Feki F, Montiel A (2008) Heavy metal removal from aqueous solutions by activated phosphate rock. J Hazard Mater 156:412–420

Eren E (2009) Removal of heavy metal ions by Unye (Turkey) bentonite in iron and magnesium oxide-coated forms. J Hazard Mater 165:63–70

Eric B, Selma L, Ronald L (2010) Fishing activity, health characteristics and Lead exposure of Amerindian women living alongside the Beni River (Amazonian Bolivia). Int J Hyg Environ Health 213:20–40

Eze SO, Igwe JC, Dipo D (2013) Effect of particle size on adsorption of heavy metals using chemically modified and unmodified fluted pumpkin and broad-leafed pumpkin pods. Int J Biol Chem Sci 7:852–860

Feng Q, Lin Q, Gong F, Sugita F, Shoya M (2004) Adsorption of Lead and mercury by rice husk ash. J Colloid Interface Sci 278:1–8

Fu F, Wang Q (2011) Removal of heavy metal ions from wastewaters: a review. J Environ Manag 92:407–418

Haydar S, Aziz JA (2009) Coagulation–flocculation studies of tannery wastewater using cationic polymers as a replacement of metal salts. J Hazard Mater 168:1035–1040

He J, Li Y, Wang C, Zhang K, Lin D, Kong L, Liu J (2017) Rapid adsorption of Pb, Cu and Cd from aqueous solutions by cyclodextrin polymers. Appl Surf Sci 426:29–39

Hom DP, Alley MM, Bertsch P (1982) Cation exchange capacity measurement. In Communication in Soil. Sci Plant Anal 13:851–862

Hua M, Zhang S, Pan B, Zhang W, Lv L, Zhang Q (2012) Heavy metal removal from water/wastewater by nano-sized metal oxides: a review. J Hazard Mater 211–212:317–331

Husein DZ (2013) Adsorption and removal of mercury ions from aqueous solution using raw and chemically modified Egyptian mandarin peel. Desalin Water Treat 51:6761–6769

Janaki RSG, Sreenivas K, Sivasamy R (2014) Hyperspectral analysis of clay minerals. Int Arch Photogr Remote Sens Spat Inf Sci 40:443–446

Jha MK, Kumar VJ, Singh R (2001) Review of hydrometallurgical recovery of zinc from industrial wastes. Resour Conserv Recycl 33:1–22

Jiang R, Tian J, Zheng H, Qi J, Sun S, Li X (2015) A novel magnetic adsorbent based on waste litchi peels for removing Pb(II) from aqueous solution. J Environ Manag 155:24–30

Karickhoff SW, Bailey GW (1973) Optical absorption spectra of clay minerals. Clays Clay Miner 21:59–70

Keren R (1986) Reduction of the cation-exchange capacity of goethite by take-up of hydroxy-a1 polymers. Clays Clay Miner 34:534–538

Khodadadi M, Malekpour A, Ansaritabar M (2017) Removal of Pb(II) and Cu (II) from aqueous solutions by NaA zeolite coated magnetic nanoparticles and optimization of method using experimental design. Microporous Mesoporous Mater 248:256–265

Kuncoro EP, Isnadina DRM, Darmokoesoemo H, Fauziah OR, Kusuma HS (2018) Characterization, kinetic, and isotherm data for adsorption of Pb^{2+} from aqueous solution by adsorbent from mixture of bagasse-bentonite. Data Brief 16:622–629

Liu Q, Li F, Lu H, Li M, Liu J, Zhang S, Sun Q, Xiong L (2018) Enhanced dispersion stability and heavy metal ion adsorption capability of oxidized starch nanoparticles. Food Chem 242:256–263

Lopez-Mũnoz MJ, Aguado J, Arencibia A, Pascuala R (2011) Lead removal from aqueous solutions of PbCl2 by heterogeneous photo catalysis with $TiO_{2'}$. Appl Catal B Environ 104:220–228

Lowell S, Shields JE (1991) Powder surface area and porosity. Springer, Amsterdam, p 252

Maity J, Ray SK (2018) Chitosan based nano composite adsorbent—synthesis, characterization and application for adsorption of binary mixtures of Pb(II) and Cd(II) from water. Carbohydr Polym 182:159–171

Maruthupandy M, Zuo Y, Chen J-S, Song J-M, Niu H-L, Mao C-J, Zhang S-Y, Shen Y-H (2017) Synthesis of metal oxide nanoparticles (CuO and ZnO NPs) via biological template and their optical sensor applications: the key laboratory of environment friendly. Appl Surf Sci 397:167–174

Ndabigengesere A, Narasiah KS (2010) Use of moringa oleifera seeds as a primary coagulant in wastewater treatment. Environ Technol 19:789–800

Nguyen TC, Loganathan P, Nguyen TV, Vigneswaran S, Kandasamy J, Naidu R (2015) Simultaneous adsorption of Cd, Cr, Cu, Pb, and Zn by an iron-coated Australian zeolite in batch and fixed-bed column studies. Chem Eng J 270:393–404

Olivaa J, De Pablo J, Cortina J-L, Cama J, Ayora C (2011) Removal of cadmium, copper, nickel, cobalt and Lead from water by Apatite IITM: column experiments. J Hazard Mater 194:312–323

Phiwdang K, Suphankij S, Mekprasart W, Pecharap W (2013) Synthesis of CuO nanoparticles by precipitation method using different precursors. Energy Procedia 34:740–745

Pirveysian M, Ghiaci M (2018) Synthesis and characterization of sulfur functionalized grapheme oxide nanosheets as efficient sorbent for removal of Pb^{2+}, Cd^{2+}, Ni^{2+} and Zn^{2+} ions from aqueous solution: a combined thermodynamic and kinetic studies. Appl Surf Sci 428:98–109

Plescia P, Maccari D (1996) Recovering metals from red mud by thermal treatment and magnetic separation. J Miner Metals Mater Soc 48:25–28

Qiu H, Lu LV, Bing-cai PAN, Qing-jian Z, Wei-ming Z, Quan-xing Z (2009) Critical review in adsorption kinetic models. J Zhejiang Univ Sci A 10:716–724

Ravichandran M (2004) Interactions between Lead and dissolved organic matter - a review. Chemosphere 55:319–331

Rivas J, Beltrán F, Carvalho F, Acedo B, Gimeno O (2004) Stabilized leachates: sequential coagulation–flocculation and chemical oxidation process. J Hazard Mater 116:95–102

Romero M, Rincón JM (1999) Surface and bulk crystallization of glass-ceramic in the Na_2O-CaO-ZnO-PbO-Fe_2O_3-Al_2O_3-SiO_2 system derived from a goethite waste. J Ame Ceram Soc 82:1313–1317

Rwiza MJ, Oh S-Y, Kim K-W, Kim SD (2018) Comparative sorption isotherms and removal studies for Pb(II) by physical and thermochemical modification of low-cost agro-wastes from Tanzania. Chemosphere 195:135–145

Saleh TA, Rachman IB, Ali SS (2017a) Tailoring hydrophobic branch in polyzwitterionic resin for simultaneous capturing of Hg(II) and methylene blue with response surface optimization. Chem Eng J 307:230–238

Saleh TA, Seri A, Tuzen M (2017b) Optimization of parameters with experimental design for the adsorption of mercury using polyethyleneimines modified-activated carbon. J Environ Chem Eng 5:1079–1088

Seema KM, Mamba BB, Njuguna J, Bakhtizin RZ, Mishra AK (2018) Removal of Lead (II) from aqeouos waste using (CD-PCL-TiO2) bio-nanocomposites. Int J Biol Macromol 109:136–142

Sharifpour E, Zare H, Ghaedi KM, Asfaram A, Jannesar R (2018) Isotherms and kinetic study of ultrasound-assisted adsorption of malachite green and Pb^{2+} ions from aqueous samples by copper sulfide nanorods loaded on activated carbon: experimental design optimization. Ultrason Sonochem 40:373–382

Shen Z, Zhang Y, Jin F, McMillan O, Al-Tabbaa A (2017) Qualitative and quantitative characterisation of adsorption mechanisms of Lead on four biochars. Sci Total Environ 609:1401–1410

Shen Z, Tian D, Zhang X, Tang L, Su M, Zhang L, Li Z, Hu S, Hou D (2018) Mechanisms of biochar assisted immobilization of Pb^{2+} by bioapatite in aqueous solution. Chemosphere 190:260–266

Stephan B, McCarty KM, Nadine S, Beate L (2010) Lead exposure and children's health. Curr Prob Pediatr Adolesc Health Care 40:186–215

Strange ED, Onwulata CI (2002) Effect of particle size on the water sorption properties of cereal fibers. J Food Qual 25:63–73

Taghipour T, Karimipour G, Ghaedi M, Asfaram A (2018) Mild synthesis of a Zn(II) metal organic polymer and its hybrid with activated carbon: application as ntibacterial agent and in water treatment by using sonochemistry: Optimization, kinetic and isotherm study. Ultrason Sonochem 41:389–396

Taraba B, Bulavová P (2018) Adsorption enthalpy of Lead(II) and phenol on coals and activated carbon in the view of thermodynamic analysis and calorimetric measurements. J Chem Thermodyn 116:97–106

Tavares FO, Pinto LAD, Bassetti FDJ, Bergamasco R, Vieira AMS (2017) Environmentally friendly biosorbents (husks, pods and seeds) from Moringa oleifera for Pb(II) removal from contaminated water. Environ Technol 38:3145–3155

Tipre DR, Dave SR (2004) Bioleaching process for Cu–Pb–Zn bulk concentrate at high pulp density. Hydrometallurgy 75:37–43

Tkacova K, Misura BM, Vigddergauz VE, Chanturiya VA (1993) Selective leaching of zinc from mechanically activated complex Cu-Pb-Zn concentrate. Hydrometallurgy 33:291–300

Uddin MK (2017) A review on the adsorption of heavy metals by clay minerals, with special focus on the past decade. Chem Eng J 308:438–462

van der Sloot HA (1991) 'Systematic leaching behavior of trace elements from construction materials and waste material's. Stud Environ Sci 48:19–36

Wang D, Lin Z, Wang T, Yao Z, Qin M, Zheng S, Lu W (2016) 'Where does the toxicity of metal oxide nanoparticles come from: the nanoparticles, the ions, or a combination of both?' Journal of Hazard. Materials 308:328–334

Wang J, Zeng G, Huang D, Hu L, Xu P, Huang C, Deng R, Xue W, Lai C, Zhou C, Wang Y, Li L, Luo C, Wang X, Duan H (2018) Removal of Pb^{2+} from water environment using a novel magnetic chitosan/graphene oxide imprinted Pb^{2+}. Int J Biol Macromol 86:505–511

Zaki AA, Ahmad MI, Abd El-Rahma KM (2017) Sorption characteristics of a landfill clay soil as a retardation barrier of some heavy metals. Appl Clay Sci 135:150–167

Zhang Y, Cao B, Zhao L, Sun L, Gao Y, Li J, Yang F (2018) Biochar-supported reduced graphene oxide composite for adsorption and co-adsorption of atrazine and Lead ions. Appl Surf Sci 427:147–155

Zhengn K, Renm X, Gong X (2018) Rhamnolipid stabilized nano-chlorapatite: synthesis and enhancement effect on Pb-and Cd-immobilization in polluted sediment. J Hazard Mater 343:332–339